Neuronal cotransport of glycine receptor and the scaffold protein gephyrin

Christoph Maas, Nadia Tagnaouti, Sven Loebrich, Bardo Behrend, Corinna Lappe-Siefke, and Matthias Kneussel

Zentrum für Molekulare Neurobiologie Hamburg, Universität Hamburg, D-20251 Hamburg, Germany

The dynamics of postsynaptic receptor scaffold formation and remodeling at inhibitory synapses remain largely unknown. Gephyrin, which is a multimeric scaffold protein, interacts with cytoskeletal elements and stabilizes glycine receptors (GlyRs) and individual subtypes of γ-aminobutyric acid A receptors at inhibitory postsynaptic sites. We report intracellular mobility of gephyrin transports packets over time. Gephyrin units enter and exit active synapses within several minutes. In addition to previous reports of GlyR–gephyrin interactions at plasma membranes, we show cosedimentation and coimmunoprecipitation of both proteins from vesicular fractions. Moreover, GlyR and gephyrin are cotransported within neuronal dendrites and further coimmunoprecipitate and colocalize with the dynein motor complex. As a result, the blockade of dynein function or dynein–gephyrin interaction, as well as the depolymerization of microtubules, interferes with retrograde gephyrin recruitment. Our data suggest a GlyR–gephyrin–dynein transport complex and support the concept that gephyrin–motor interactions contribute to the dynamic and activity-dependent rearrangement of postsynaptic GlyRs, a process thought to underlie the regulation of synaptic strength.

Introduction

Postsynaptic scaffolds are thought to be crucial for receptor immobilization at both excitatory and inhibitory synapses (Kennedy, 2000; Kneussel and Betz, 2000; Moss and Smart, 2001; Sanes and Lichtman, 2001; Li and Sheng, 2003). Synaptic receptor–scaffold complexes interact with different cytoskeletal elements (Kirsch and Betz, 1995; Passafaro et al., 1999; Giesemann et al., 2003). These interactions stabilize the complex and are thought to participate in the entry and exit of receptors and/or scaffold elements at postsynaptic sites (Choquet and Triller, 2003). At inhibitory synapses, gephyrin represents a core protein on the cytoplasmic side of the postsynaptic plasma membrane. Gephyrin harbors two oligomerization domains and is thought to generate a reversible postsynaptic scaffold for the immobilization of glycine receptors (GlyRs) and individual subtypes of γ-aminobutyric acid A receptors ($GABA_AR$s; Kneussel and Betz, 2000; Sola et al., 2004). Structural analysis of both gephyrin's oligomerization and GlyRβ subunit binding sites revealed that dimeric gephyrin interacts with GlyRβ subunits and that subsequent multimerization is required to form a hexagonal gephyrin lattice (Kneussel and Betz, 2000; Sola et al., 2004). Consequently, disassembly of the gephyrin scaffold must occur to enable dynamic changes at the postsynaptic specialization.

Long distance intraneuronal transport of neurotransmitter receptors and associated proteins is typically mediated by microtubule-based motor complexes (Hirokawa and Takemura, 2005). Notably, individual synapse-associated proteins, which locate at postsynaptic densities, are reported to act as adaptor proteins between neurotransmitter receptors and motor protein complexes (Setou et al., 2000, 2002; Kneussel, 2005). For instance, the glutamate receptor–interacting protein 1 (GRIP1) functions as a transport adaptor that links intracellular α-amino-3-hydroxy-5-methyl-4-isoxazolepropionate (AMPA) receptor GluR2 subunits to the kinesin superfamily motor KIF5 (Setou et al., 2002). Moreover, GRIP1 binds to plasma membrane–inserted AMPA receptors at the postsynaptic specialization (Dong et al., 1997; Wyszynski et al., 1998), suggesting a dual role for receptor-associated proteins in transport and postsynaptic scaffold reactions. The use of a common set of proteins for both transport and plasma membrane anchoring may contribute to transport specificity and postsynaptic integration or to removal

C. Maas and N. Tagnaouti contributed equally to this paper.

Correspondence to Matthias Kneussel: matthias.kneussel@zmnh.uni-hamburg.de

Abbreviations used in this paper: AMPA, α-amino-3-hydroxy-5-methyl-4-isoxazolepropionate; DHC, dynein heavy chain; DIC, dynein intermediate chain; DLC, dynein light chain; $GABA_AR$, γ-aminobutyric acid A receptor; GlyR, glycine receptor; GRIP1, glutamate receptor–interacting protein 1; HEK, human embryonic kidney; mRFP, monomeric red fluorescent protein; MTOC, microtubule-organizing center; NMDA, *N*-methyl-D-asparate; VIAAT, vesicular inhibitory amino acid transporter.

The online version of this article contains supplemental material.

The Journal of Cell Biology, Vol. 172, No. 3, January 30, 2006 441–451
http://www.jcb.org/cgi/doi/10.1083/jcb.200506066

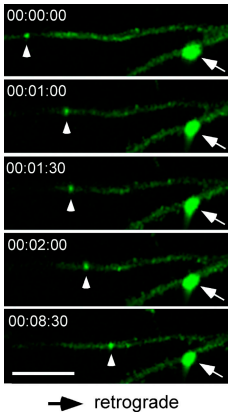

Figure 1. **Gephyrin transport units are rapidly recruited in dendrites of cultured hippocampal neurons.** A small gephyrin particle (arrowhead) moved in a retrograde direction toward a dendritic branch point over time. In contrast, a larger gephyrin aggregate on the other branch (arrow) was immobile. Bar, 5 μm.

of receptors that underlie synapse formation and plasticity (Kneussel, 2005).

We investigated the dynamics of gephyrin and show that intracellular gephyrin forms a transport complex with inhibitory GlyR and the dynein motor. Our data suggest that this triple complex participates in receptor–scaffold dynamics at inhibitory synapses.

Results

Gephyrin particles are mobile

To examine whether gephyrin particles are subjects of active transport in dendrites, time-lapse video microscopy was applied on cultured hippocampal neurons from different developmental stages expressing a previously described GFP–gephyrin fusion protein (Fuhrmann et al., 2002). In mature neurons cultured for 12–14 d in vitro, gephyrin autofluorescent particles were recruited within dendrites in both the anterograde and retrograde direction (Fig. 1 and not depicted). Particle movement was observed in a discontinuous manner, with alternate mobility and immobility of particles over time. A quantitative evaluation of GFP–gephyrin transport packets revealed on average only 1.8 mobile particles per cell during image acquisition, a value that represents 2.2% of the total clusters. Control stainings with the synaptic marker SV2 (Feany et al., 1992) confirmed the maturity of the culture, as indicated by the high density of synaptic contacts (unpublished data). Notably, the number of mobile particles in our system is consistent with data published by Lorenzo et al. (2004), which show that 2% of gephyrin-positive immunogold particles locate in the neuronal cytoplasm, whereas the majority of gephyrin is associated with submembrane regions. GFP–gephyrin clusters were transported at mean velocities of 1.3 ± 0.1 μm/min, a value that resembles the transport characteristics of the postsynaptic density protein PSD-95 (Marrs et al., 2001; Washbourne et al., 2002). To test whether the recruitment of gephyrin particles represents active transport or diffusion processes, we applied time-lapse microscopy with image acquisition rates of 1 frame/s (unpublished data). As indicated by the absence of undirected movement, we concluded that active transport processes, but not diffusion, drive gephyrin particle recruitment in our system.

Transport packets enter and leave postsynaptic gephyrin scaffolds at active synapses

Two gephyrin particle populations of different sizes were prominent within neurites. Notably, only the small fluorescent particles were mobile and frequently added to larger immobile particles (Fig. 2 A and Video 1, available at http:/www.jcb.org/cgi/content/full/jcb.200506066/DC1). In addition, small-sized particles left immobile clusters over time (Fig. 2 B). An evaluation of the relative size of GFP–gephyrin particles in the culture system revealed that mobile particles are on average ~2.6-fold smaller compared with immobile particles (Fig. 2 C). Therefore, we hypothesized that mobile particles might represent gephyrin

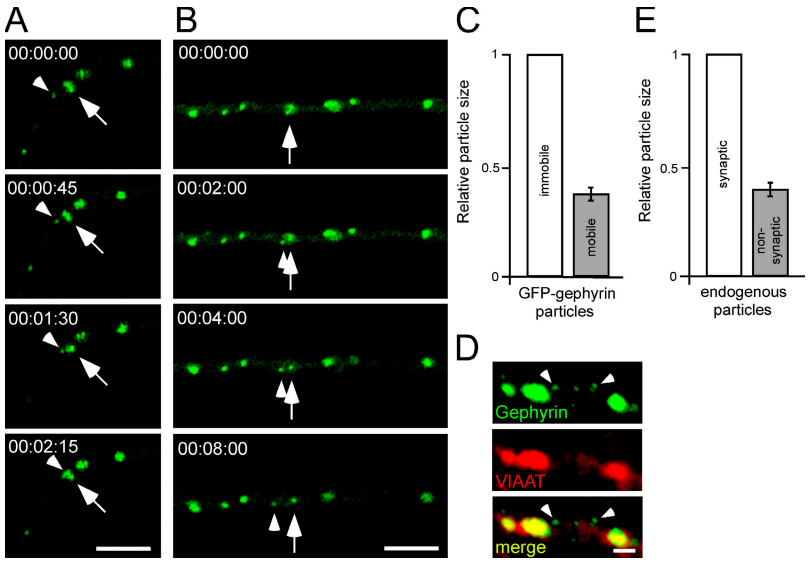

Figure 2. **Recruitment of GFP–gephyrin transport units to and from sites of immobile gephyrin clusters.** Images were acquired every 30 or 45 s. (A) Small particle recruitment (arrowhead) toward a larger immobile gephyrin cluster (arrow). (B) A small cluster (arrowhead) left an immobile site of gephyrin autofluorescence (arrow) over time. Note that the shift in focus is caused by temperature variations during image acquisition. (C) Relative particle size of immobile and mobile GFP–gephyrin puncta. (D) Detection of two populations of endogenous gephyrin clusters within dendrites with a significant size difference. Large endogenous gephyrin clusters (green) colocalized with the presynaptic marker VIAAT (red), as represented in the merged image (yellow). In contrast, small clusters, which were frequently mobile in time-lapse experiments, did not colocalize with presynaptic terminal boutons (arrowheads). (E) Relative particle size of synaptic and nonsynaptic endogenous gephyrin puncta. Error bars represent size variations of mobile clusters, as compared with immobile clusters. Bars: (A and B) 5 μm; (D) 2 μm.

transport units participating in size increase and reduction of preexisting postsynaptic gephyrin scaffolds. To test this, we applied immunostaining against endogenous gephyrin and the vesicular inhibitory amino acid transporter (VIAAT), which is a marker labeling inhibitory presynaptic terminals. In this assay, large endogenous gephyrin aggregates exclusively colocalized with presynaptic boutons (Fig. 2 D), indicating that this particle population indeed represents gephyrin scaffolds at mature postsynaptic sites (Kneussel and Betz, 2000). In contrast, no colocalization with synaptic marker was obtained for small-size particles (Fig. 2 D), which were frequently mobile in our system. Endogenous gephyrin clusters at nonsynaptic sites were on average 2.3-fold smaller than synaptic clusters (Fig. 2 E). For the simultaneous detection of both axon-terminal boutons and gephyrin in living neurons, we loaded GFP–gephyrin–expressing neurons with FM4-64 dye, which visualizes synaptic vesicle recycling and is therefore indicative of synaptic activity (Washbourne et al., 2002). As seen in Fig. 3 A, gephyrin transport units emerged from active synaptic contacts (yellow) and merged with other FM4-64–positive terminal boutons over a time period of several minutes (Fig. 3, A and B). Notably, the mobile particle moved relatively fast between the individual synaptic contacts, but was delayed at active FM4-64–labeled presynaptic sites (Video 2). Together, these data suggest that intracellular transport processes recruit the gephyrin transport units underlying postsynaptic scaffold remodeling at inhibitory synapses.

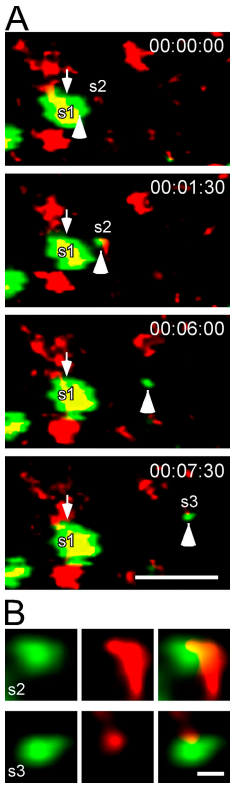

Figure 3. **Recruitment of gephyrin transport packets from and to active synapses.** Cultures were supplemented with FM4-64 dye (red) to visualize active presynaptic terminal boutons. Pre- and postsynaptic appositions are depicted as s1–s3. Colocalization of GFP–gephyrin– (green) and FM4-64–positive terminals (red) is represented in yellow. (A) A gephyrin transport packet (arrowhead), which emerged from synapse s1 (arrow), rapidly merged with/emerged from other synapses. Over a total time period of ~7 min, the mobile gephyrin packet colocalized with different active terminal boutons. Note that loss or appearance of individual red fluorescent puncta is because of the flexibility of individual axon terminals within the culture system and subsequent shift in focus during image acquisition. (B) Magnification of synapses s2 and s3 from A. Bars: (A) 5 μm; (B) 0.2 μm.

GlyR and gephyrin cotransport

Because gephyrin is a direct binding partner of plasma membrane GlyRβ subunits (Schmitt et al., 1987), we asked whether gephyrin and GlyR could be subjects of intracellular cotransport. Because 98% of neuronal gephyrin locates at plasma membrane regions (Lorenzo et al., 2004), we first examined whether gephyrin associates with intracellular vesicle fractions at all (Saito et al., 1997). Sucrose gradient centrifugation on 160,000 *g* vesicle-enriched pellets revealed that GlyR sedimentation peaked around 1.6 M, a molarity that is highly enriched with gephyrin immunoreactivity (Fig. 4, A and B). Consistent with an intracellular GlyR–gephyrin association, we also obtained in vitro binding of GlyR and gephyrin from cytoplasmic vesicle–rich fractions using either GlyR- or gephyrin-specific antibodies for precipitation (Fig. 4 C). Intracellular GlyR–gephyrin complexes should not colocalize with synaptic markers. To address whether one could identify small puncta of GlyR and gephyrin coimmunoreactivity that do not represent synaptic cluster formations, we immunostained cultured hippocampal neurons known to contain synaptic GlyR (Danglot et al., 2004; Fig. S1 A, available at http://www.jcb.org/cgi/content/full/jcb.200506066/DC1) against endogenous gephyrin, GlyR, and synaptophysin. Indeed, small GlyR–gephyrin–colocalized puncta, which likely represent en route transport particles, were frequently identified at nonsynaptic regions (Fig. 4 D), suggesting that these particles are the subjects of cotransport. A quantitative evaluation revealed ~90% colocalization of GlyR and gephyrin clusters in this system, with 81% of these coclusters locating at synaptophysin-positive synapses (Fig. 4 E). This finding indicates that ~20% of GlyR–gephyrin coclusters are nonsynaptic, a value that includes candidate particles in transit. To confirm cotransport of both particles in a living system, we expressed fluorescent fusion proteins in the cultured neurons monomeric red fluorescent protein (mRFP)–gephyrin and GFP–GlyRβ and performed double-channel time-lapse video microscopy. Both fusion proteins formed clusters in distal neurites, were recognized by GlyR- or gephyrin-specific antibodies, and displayed strong colocalization (Fig. 5 A and Fig. S1 B). Indeed, mRFP–gephyrin transport units comigrated together with GFP–GlyRβ particles over time, indicating an intracellular transport complex of both proteins (Fig. 5 B and Video 3).

The intracellular recruitment and/or transport of individual synaptic proteins can be regulated in an activity-dependent manner. This includes the synaptic localization of profilin I and II (Ackermann and Matus, 2003; Neuhoff et al., 2005), which are both factors that interact with actin and gephyrin. Moreover, neuronal depolarization alters the phosphorylation state of MAP2 and, consequently, the stability of microtubules (Quinlan and Halpain, 1996), which represent tracks for intraneuronal transport. To test whether alterations of electrical parameters functionally influence GlyR–gephyrin cotransport, we depolarized

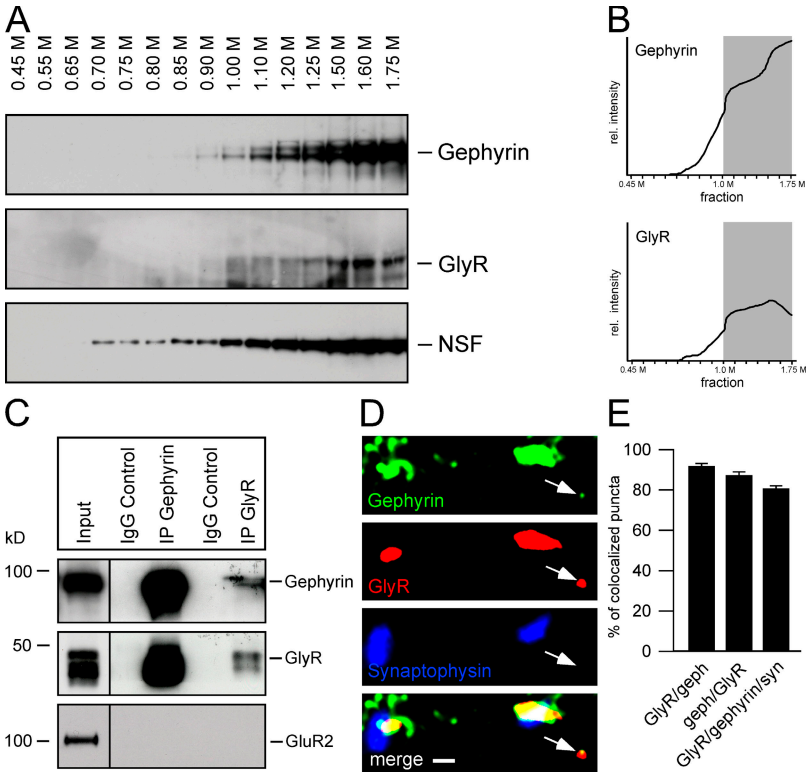

Figure 4. **Association of gephyrin and GlyR at cytoplasmic vesicle-rich cell compartments.** (A) Cosedimentation of gephyrin and GlyR upon sucrose gradient centrifugation of 160,000 *g* vesicle-enriched pellets. NSF detection was used as a loading control. (B) The majority of gephyrin and GlyR immunoreactivity is detected above the 1.0-M fraction. (C) Coimmunoprecipitation on rat brain cytoplasmic vesicle–enriched cell fractions using both gephyrin- and GlyR-specific antibodies. Beads coupled with antibody, but not with control IgG, retain gephyrin and GlyR, but not GluR2. (D) Triple detection of endogenous gephyrin, GlyR, and the synaptic marker synaptophysin in dendrites of cultured hippocampal neurons. In contrast to synaptic sites (white), individual small-size nonsynaptic puncta display GlyR–gephyrin colocalization (yellow; arrows). These particles represent putative molecules in transit. (E) Quantitative evaluation of colocalized puncta. Error bars represent variations between individual experiments. Bar, 1.5 μm.

cultures with physiological concentrations of KCl and/or applied the GlyR-specific antagonist strychnine during time-lapse analysis. Notably, the average velocity of GFP–gephyrin particle transport increased significantly either when cultures were depolarized or when GlyR function was blocked (Fig. 5 C). Also, the combined parameters (KCl + strychnine) resulted in an increase of average particle velocity, as compared with control conditions. In addition, strychnine-mediated GlyR blockade, but neither KCl-mediated depolarization nor bicuculline-mediated $GABA_AR$ blockade, caused a significant increase in the average number of mobile GFP–gephyrin particles (Fig. 5 C). This observation was accompanied by a shift from anterograde to retrograde transport in the presence of strychnine (Fig. 5 C), suggesting that GlyR inactivity, but not KCl-mediated neuronal depolarization, causes retrograde GlyR–gephyrin removal from synaptic sites. In accordance with this finding are previous observations, in which chronic GlyR blockade through the antagonist strychnine over several days caused a recruitment of GlyR clusters toward neuronal somata in cultured neurons (Kirsch and Betz, 1998; Levi et al., 1998). Together, these results provide functional evidence for an activity-dependent component regulating GlyR–gephyrin cotransport, as GlyR blockade not only alters GlyR recruitment but also the recruitment of comigrating gephyrin polypeptides. They further suggest a molecular motor system representing the driving force for neuronal recruitment of this complex.

Gephyrin derived from intracellular fractions binds the dynein motor complex

Gephyrin interacts with dynein light chains (DLCs; Fuhrmann et al., 2002); however, as these polypeptides represent components of both dynein and myosin motors, it could not be predicted whether gephyrin associates with one motor system or the other. Therefore, we performed coimmunoprecipitation with 400,000 *g* pellets using antibodies specific for gephyrin and 74-kD dynein intermediate chains (DICs), the latter representing exclusive components of the dynein motor complex (Harrison and King, 2000). Endogenous gephyrin was specifically enriched in the precipitate, but was not detectable when unspecific immunoglobulins were used. In addition, the use of control IgG and two independent antibodies directed against DIC revealed specific coimmunoprecipitation of DIC with the gephyrin complex (Fig. 6 A and not depicted), indicating that both gephyrin and DIC are components of the same complex. Triple labeling of endogenous proteins also confirmed dynein association and further revealed that sites of dynein–gephyrin or dynein–GlyR colocalization are occasionally found close to, but mainly not at, synaptic sites, suggesting that they represent molecules in transit (Fig. 6 B). In accordance with our quantitative evaluation in Fig. 4 E, this observation was obtained under experimental conditions with ~80% of GlyR or gephyrin clusters in colocalization with either synaptophysin or the VIAAT marker, respectively. As a control for our time-lapse experiments, we also expressed GFP–gephyrin fusion proteins in cultured hippocampal neurons and analyzed colocalization with the dynein motor complex. Consistently, individual GFP–gephyrin particles are also found in colocalization with the 74-kD DIC in dendrites (Fig. S1 C).

To test whether GlyRs, gephyrin, and dynein are associated in a triple complex formation, we performed immunoprecipitation using GlyR-specific antibodies. Immunodetection of the individual binding partners, as immobilized on the same

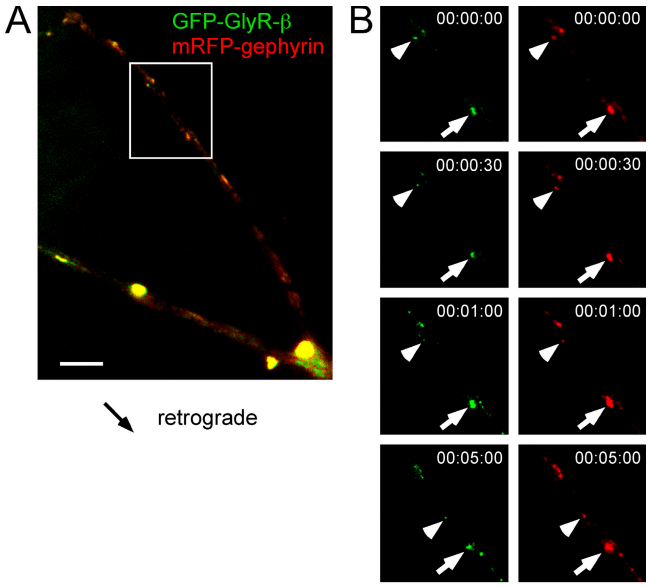

C

GFP-gephyrin	Control (n=49)	KCl (n=60)	strychnine (n=44)	KCl+strychnine (n=81)	KCl+bicuculline (n=41)
Average velocity (μm/min)	1.3	2.3	2.8	2.2	2.4
Average number of mobile clusters/cell	1.8	1.7	4.0	3.9	1.5
Anterograde movement	51%	49%	25%	24%	51%
Retrograde movement	49%	51%	75%	76%	49%

Figure 5. **Cotransport of gephyrin and GlyRβ subunits in cultured hippocampal neurons.** (A) Neuronal coexpression of GFP–GlyRβ and mRFP–gephyrin. Both fusion proteins cluster and colocalize in dendrites. (B) Time-lapse video microscopy revealed cotransport of both puncta over time. Two particles in each fluorescent channel (arrowheads) are recruited in the retrograde direction toward the dendritic branch point shown in A. An immobile cluster of GlyR–gephyrin coimmunoreactivity is indicated by arrows. (C) GFP–gephyrin transport particle characteristics upon 10 mM KCl-induced neuronal depolarization and/or application of the GlyR and $GABA_AR$ antagonists strychnine and bicuculline, respectively. Velocity changes upon KCl or strychnine application and the shift toward retrograde movement upon strychnine application are significant ($P < 0.001$), as compared with control values. Bar, 5μm.

membrane, revealed that GlyR was specifically precipitated and that both gephyrin and DIC, but not GluR2, were subjects of coprecipitation (Fig. 6 C). In accordance, triple immunodetection of GlyR, gephyrin, and dynein heavy chain (DHC) in cultured hippocampal neurons frequently displayed sites of triple colocalization (Fig. 6 D) with ~13.5% of GlyR and/or gephyrin puncta colocalizing with DHC, as compared with 5.7% colocalization with an unrelated control (Fig. 6 E; $P < 0.001$). Together, our data indicate the existence of a transport complex consisting of gephyrin functioning as an adaptor protein that couples vesicular GlyR with the dynein motor complex (Fig. 6 F).

Functional blockade of dynein-mediated gephyrin transport

Dynein motor complexes mediate a variety of functions in neurons (Guzik and Goldstein, 2004; Holzbaur, 2004). To show a direct and functional link between gephyrin transport and dynein-mediated reactions, we initially searched for a cell system with less complexity. Remarkably, gephyrin does not

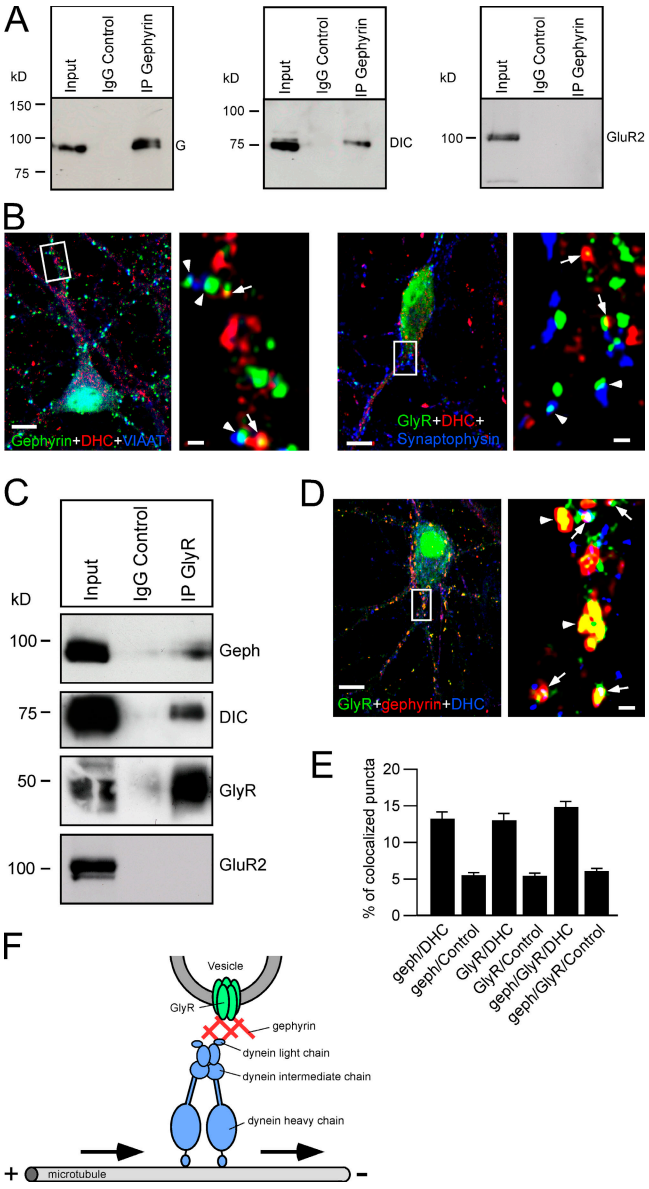

Figure 6. **Formation of a GlyR–gephyrin–dynein triple complex.** (A) Coimmunoprecipitation of gephyrin and the 74-kD DIC, which is retained from beads coupled with monoclonal gephyrin antibody, but not coupled with control IgG. GluR2 detection serves as a negative control. (B) Colocalization of endogenous gephyrin or GlyR (green) with DHC (red) and synapse markers (blue) in neuronal dendrites. Magnifications of insets are shown to the right of the images. Note that putative molecules in transit locate at nonsynaptic sites (arrows). Synaptic sites are marked by arrowheads. (C) Triple coimmunoprecipitation experiment. Beads coupled with GlyR-specific antibody, but not coupled with control IgG, retain GlyR, gephyrin, and DIC, but not GluR2. (D) Immunocytochemical detection of endogenous GlyR, gephyrin, and DHC. Note that triple complex formations (white, arrows) are putative transport molecules. Large yellow clusters represent GlyR–gephyrin colocalization at putative synapses (arrowheads). Magnification of the inset is shown to the right of the image. (E) Quantitative evaluation of gephyrin, GlyR, and DHC colocalization experiments shown in B and D. Values are significantly ($P < 0.001$) above colocalization values obtained with the unrelated motor protein KIF1B. (F) Schematic representation of the GlyR–gephyrin–dynein transport complex. Bars: (B and D) 5 μm; (B and D, magnifications) 0.5 μm.

reach the plasma membrane compartment upon heterologous expression in human embryonic kidney 293 (HEK293) cells, but rather accumulates in intracellular aggregates (Fuhrmann et al.,

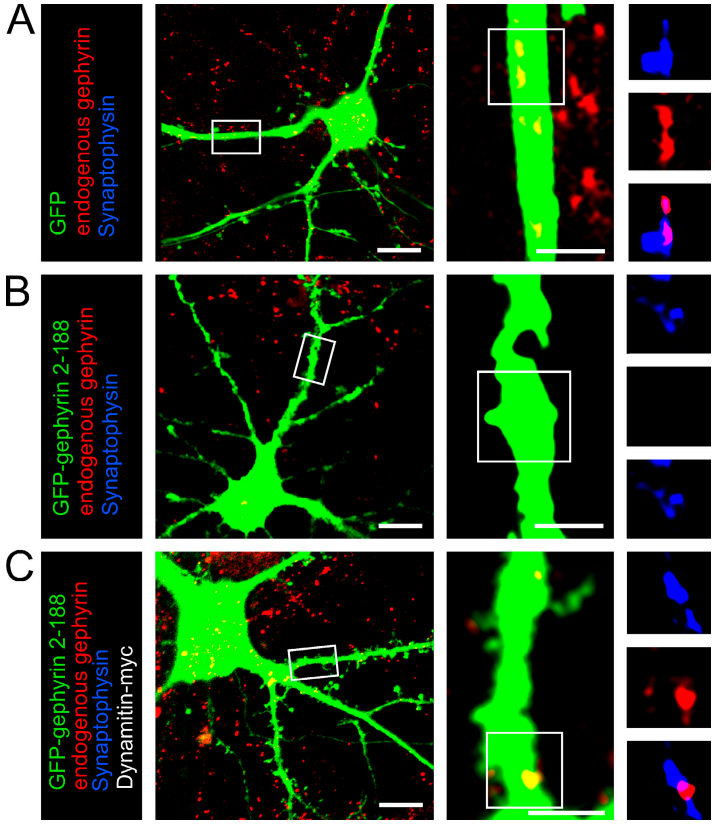

Figure 7. **Inhibition of dynein-mediated transport in neurons.** The blockade of dynein motor function prevents the dominant-negative–induced loss of synaptic gephyrin clusters in cultured hippocampal neurons. (A–C) Boxed regions are shown at higher magnification. Yellow indicates fluorescent overlap of endogenous gephyrin (red) and GFP or GFP-fusion protein (green). The magenta color represents fluorescent overlap of gephyrin (red) and synaptic sites (blue). Red aggregates outside the fluorescent cell (green) represent gephyrin clusters of nontransfected cells within the culture. (A) Control condition visualizing synaptic gephyrin clusters in GFP-expressing neurons. (B) Upon overexpression of a dominant-negative construct fused to GFP (GFP–gephyrin 2–188), preexisting gephyrin clusters are lost in neurite processes. (C) Dynamitin-induced inhibition of dynein motor function prevents loss of preexisting gephyrin clusters in the presence of the dominant-negative construct described in B. Remaining gephyrin clusters are localized at synaptic sites. Synapses are represented by synaptophysin immunoreactivity. Bars: (A–C) 15 μm; (A–C, magnifications) 5 μm.

2002). We hypothesized that HEK293 cells may lack the appropriate anterograde transport system to recruit gephyrin toward the plasma membrane. In this case, dynein-mediated retrograde transport reactions could accumulate gephyrin polypeptides at the microtubule-organizing center (MTOC), which harbors the minus ends of microtubules. Indeed, double detection of heterologously expressed YFP–gephyrin and endogenous γ-tubulin, representing a marker for MTOCs (Oakley and Akkari, 1999), revealed that intracellular gephyrin aggregates highly colocalized with MTOC structures (Fig. S2, available at http://www.jcb.org/cgi/content/full/jcb.200506066/DC1). In contrast, by overexpressing dynamitin, which represents a widely used blocker of dynein motor function (Burkhardt et al., 1997), gephyrin aggregates were no longer found at MTOCs (Fig. S2). Therefore, we conclude that gephyrin tends to aggregate in this cell type because of its multimerization domains (Sola et al., 2001, 2004). Gephyrin is further transported in microtubule minus-end directions via the dynein motor complex, and the blockade of dynein-mediated transport relocalizes gephyrin aggregates within the cytoplasm of these nonneuronal cells.

Next, we aimed to inhibit dynein function in neurons. Based on structural observations on the gephyrin polypeptide (Sola et al., 2001, 2004), we expressed an NH_2-terminal truncated gephyrin polypeptide (amino acids 2–188) fused to GFP in mature cultured hippocampal neurons. This polypeptide harbors the trimerization motif, but lacks the dimerization motif of gephyrin and therefore represents a dominant-negative protein. Thus, this gephyrin deletion mutant interferes with the incorporation of endogenous gephyrin into a hexagonal scaffold formation (Sola et al., 2004), thereby reducing gephyrin cluster stability over time. As a result, cells that highly express this deletion mutant are represented by loss of endogenous gephyrin clusters in neurites within 24 h of expression, with very few aggregates remaining in the cell somata (Fig. 7 B). Based on the hypothesis that postsynaptic gephyrin cluster formation and/or remodeling is a constant steady-state process (Figs. 2 and 3) that involves dynein-mediated retrograde transport reactions, the GFP–gephyrin 2–188 mutant was coexpressed together with the dynein transport inhibitor dynamitin (Burkhardt et al., 1997). A control of dynamitin function in hippocampal neurons is shown in Fig. S3 (A and B, available at http:/w.jcb.org/cgi/content/full/jcb.200506066/DC1). Notably, dynamitin overexpression prevented the dominant-negative–induced loss of endogenous gephyrin clusters, which remained at synaptic sites under these conditions (Fig. 7 C). These results are likely to depend on a severe slowdown of gephyrin scaffold turnover upon dynein inhibition, which prevents the incorporation of truncated polypeptides (encoded by GFP–gephyrin 2–188) into preexisting gephyrin scaffold formations and, thus, the loss of endogenous gephyrin clusters. In any case, we show for the first time a functional requirement of dynein for gephyrin recruitment in neurons.

Dynein-dependent transport processes require microtubules as tracks for transport, and the depolymerization of microtubules interferes with dynein-dependent cargo recruitment in both neurons and other cell types (Ahmad et al., 1998). To analyze whether the depolymerization of microtubules interferes with gephyrin transport, we also treated mature

cultured hippocampal neurons with nocodazole, a microtubule-depolymerizing agent (Samson et al., 1979). As indicated by immunocytochemistry using an α-tubulin–specific antibody, microtubules depolymerized within 15 min of nocodazole application (Fig. S4 A, available at http://www.jcb.org/cgi/content/full/jcb.200506066/DC1). By use of the assay, as shown in Fig. 7, dominant-negative–induced loss of gephyrin clusters was prevented in the absence of microtubules (Fig. S4 D), confirming that gephyrin recruitment is also a microtubule-dependent transport process.

Inhibition of dynein transport by dynamitin causes the blockade of various dynein-dependent transport reactions. To more specifically interfere with gephyrin–dynein interactions, we generated a mRFP fusion protein (mRFP–gephyrin 181–243; Fig. 8 A) harboring the DLC-binding motif of gephyrin. This gephyrin peptide was previously shown to specifically interact with DLCs (Fuhrmann et al., 2002). Remarkably, overexpression in cultured hippocampal neurons revealed that this isolated gephyrin-derived polypeptide is able to functionally interact with the dynein motor complex, as detected by retrograde movement of mRFP fusion proteins over time (Fig. 8 B). This finding corroborates the aforementioned data indicating that dynein specifically binds and transports gephyrin. A control that overexpression of this fusion protein does not generally interfere with dynein transport is shown in Fig. S3 C, indicating that the formation of the Golgi complex (GM130 immunostaining of cis-Golgi), known to depend on functional dynein, is normal in cells that overexpress mRFP–gephyrin 181–243. We further coexpressed GFP–gephyrin and mRFP– gephyrin 181–243 in neurons to analyze whether the red fluorescent fusion protein is able to compete with binding to dynein and therefore affects retrograde transport of full-length GFP–gephyrin. As seen in Fig. 8 C, localization of full-length GFP–gephyrin clusters to distal dendrites was normal. Consistent with this, anterograde movement of full-length GFP–gephyrin particles was detectable in cells expressing both fusion proteins for ∼12 h (unpublished data). However, upon overexpression of mRFP–gephyrin 181–243, transport of full-length GFP–gephyrin particles in retrograde directions was undetectable (n [cells] = 34; n [clusters] >1,000). In contrast, mRFP fusion proteins consisting of gephyrin residues 181–243 in the same cells were highly mobile in retrograde directions (Fig. 8 C), suggesting that overexpression of the isolated binding motif competes with full-length, most likely multimerized, GFP–gephyrin for dynein interaction. Finally, upon expression of mRFP–gephyrin 181–243 for several days the anterograde transport route of GFP–gephyrin was also decreased and ultimately undetectable in neurons expressing both fluorescent proteins, thereby confirming our previous observations (Figs. 2 and 7), which suggested that gephyrin is the subject of a highly regulated turnover process including both transport directions. As a result, blockade of one transport direction also affects the opposite directed transport on a longer time scale. However, more importantly, these results indicate that an isolated DLC-binding motif of gephyrin competes with full-length GFP–gephyrin particle transport, thereby corroborating aforementioned loss-of-function results using dynamitin and nocodazole, which show that gephyrin binds the dynein motor complex via DLC interactions and is functionally transported by this molecular motor system. In accordance to these observations, combined neuronal expression of GFP–GlyRβ and mRFP–gephyrin 181–243 led to similar results (Fig. S5, available at http://www.jcb.org/cgi/content/full/jcb.200506066/DC1). Consequently, gephyrin and/or GlyR–gephyrin remodeling processes at inhibitory postsynaptic sites essentially depend on active transport via dynein.

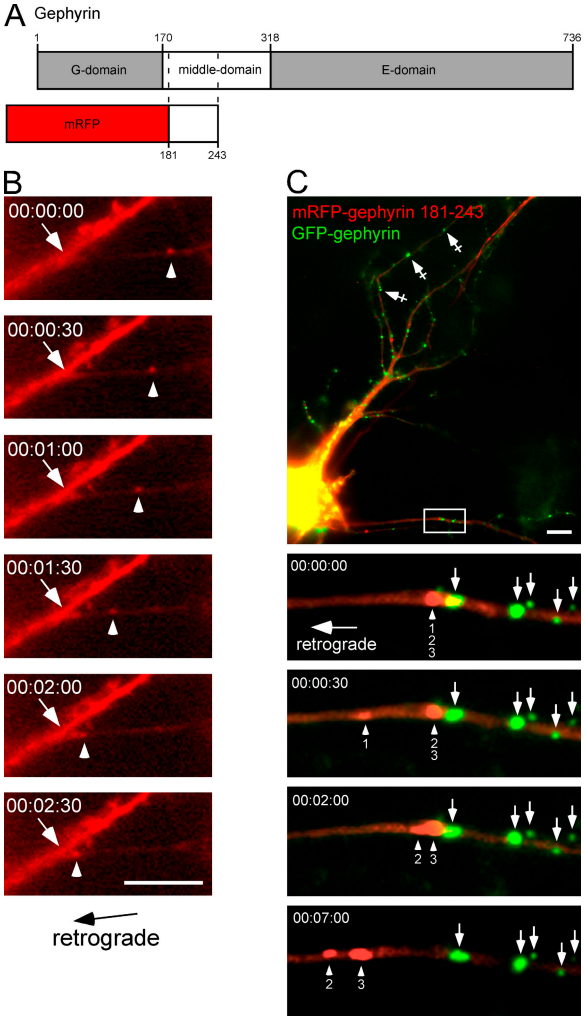

Figure 8. **Competition of dynein-mediated gephyrin transport by overexpression of the isolated DLC-binding motif of gephyrin.** (A) Schematic representation of the gephyrin domain structure (Sola et al., 2004). The DLC-binding motif, which is located between gephyrin residues 181–243 (Fuhrmann et al., 2002), is fused to mRFP (mRFP–gephyrin 181–243). (B) Singly expressed mRFP–gephyrin 181–243 fusion protein (arrowhead) is retrogradely transported toward a dendritic branch point (arrow) in cultured hippocampal neurons over time. (C) Dual-channel time-lapse recording of cultured hippocampal neurons expressing GFP–gephyrin and mRFP–gephyrin 181–243. Localization of GFP–gephyrin clusters at distal dendrites (crossed arrows), which depends on anterograde transport, is normal, whereas retrograde transport of GFP–gephyrin is inhibited. In contrast, retrograde transport of mRFP–gephyrin 181–243 is frequently observed. Note that at several days of expression, GFP–gephyrin scaffold turnover is blocked in both directions, whereas mRFP–gephyrin 181–243 remains mobile. The boxed region is shown at higher magnification. Arrows indicate immobile puncta, arrowheads indicate three mobile particles (1, 2, and 3) that subsequently move toward the cell body. Bars: (B) 3 μm; (C) 5 μm.

Discussion

Using a combination of biochemical, immunocytochemical, and time-lapse assays in neurons, we functionally investigated the dynamics of gephyrin, a scaffold component at postsynaptic specializations of inhibitory synapses. We demonstrate that gephyrin particles enter and leave active synapses in the range of minutes and can be subject of cotransport together with the inhibitory GlyR. Furthermore, the molecular motor dynein binds and colocalizes with GlyR–gephyrin transport units and functionally recruits them in a microtubule-dependent manner along neuronal processes. Our data postulate a GlyR–gephyrin–dynein transport complex that is involved in retrograde transport processes underlying postsynaptic remodeling.

As revealed in a recent electron microscopy quantitative analysis (Lorenzo et al., 2004), 86.5% of gephyrin locates at synaptic and perisynaptic regions in neurons. These values are consistent with our quantitative evaluation as shown in Fig. 4 E. Another significant proportion of gephyrin (11.5%) is also found in association with the plasma membrane at extrasynaptic sites, whereas only 2% of gephyrin locates in the cytoplasm. These values demonstrate the tendency of this polypeptide to assemble at plasma membrane regions, a process that requires multimerization through a trimerization motif in the NH_2-terminal and a dimerization motif in the COOH-terminal part of the protein (Sola et al., 2001, 2004). It has been hypothesized that gephyrin generates a reversible scaffold for postsynaptic receptor recruitment (Kneussel and Betz, 2000; Sola et al., 2004) that underlies constant exchange of material to subsequently regulate the number of receptors available for synaptic transmission (Choquet and Triller, 2003). However, until now there has been no experimental evidence for a dynamic exchange of gephyrin at synapses.

Analysis of gephyrin over time revealed that only a small percentage of particles are mobile within neurite projections. This value is consistent with small amounts of gephyrin locating in the neuronal cytoplasm (Lorenzo et al., 2004) and suggests that intracellular gephyrin represents molecules in transit. Our quantitative analysis of GlyR–gephyrin–dynein colocalization is slightly higher than the mobile particles observed; however, it has to be considered that not all transport complexes attach to microtubules at a given time (King and Schroer, 2000), a conclusion that is consistent with our observation of discontinuous movements with alternate mobility and immobility over time. The velocity of gephyrin particles ($\sim$1.3 μm/min) closely resembles the transport characteristics of PSD-95, a molecule that is also involved in scaffold formation at postsynaptic sites of excitatory synapses (Marrs et al., 2001; Washbourne et al., 2002). Notably, mobile gephyrin particles were added to or released from active synapses in the range of several minutes, suggesting that gephyrin transport is involved in fast modular assembly/remodeling of scaffold size and/or neurotransmitter receptor transport over time.

In contrast to the prominent association of gephyrin and GlyR at plasma membranes, both immunostaining and immunoprecipitation using high-speed fractions indicated that intracellular gephyrin is also associated with GlyR in the cytosol, interactions likely to represent cotransported molecules in transit. Indeed, dual-channel time-lapse analysis revealed retrograde cotransport of gephyrin and GlyR fusion proteins, thereby functionally confirming the existence of intracellular GlyR–gephyrin transport complexes.

Notably, upon addition of physiological KCl concentrations, neuronal depolarization, as well as blockade of GlyR-mediated inhibition, enhanced the transport velocities of GFP–gephyrin particles in our system, suggesting that feedback mechanisms might exist that cross talk between the neuronal surface membrane and the intracellular transport machinery. It is known that alterations in neuronal activity recruit other components to and from synapses (Fischer et al., 2000; Star et al., 2002; Ackermann and Matus, 2003; Neuhoff et al., 2005) and depolarization of neonatal hippocampal slices also increases phosphorylation of the microtubule-associated protein MAP2, thereby impairing its ability to stabilize microtubules (Quinlan and Halpain, 1996). Although the exact mechanisms are currently unknown, it is possible that activity-regulated stability of cytoskeletal elements might contribute to the velocity of cargo delivery in neurons.

Because gephyrin directly binds the inhibitory GlyR and functionally associates with $GABA_AR$ subtypes (Schmitt et al., 1987; Essrich et al., 1998; Kneussel et al., 1999), we also analyzed the transport characteristics of GFP–gephyrin in the presence of the GlyR or $GABA_AR$ antagonists strychnine or bicuculline, respectively. Although this situation is not physiological, it showed that the blockade of GlyR, but not of $GABA_AR$, affects GFP–gephyrin transport. In fact, upon GlyR blockade, the number of mobile GFP–gephyrin particles increased by $>$100% with a distinct shift of transport in the retrograde direction. Because this strychnine-mediated shift of gephyrin transport was observed both with and without KCl, it seems likely that the effects mediated by KCl and strychnine are independent of each other. Different studies have previously reported that chronic strychnine-mediated blockade of GlyR causes an intracellular receptor accumulation at neuronal somata near the nuclear compartment (Kirsch and Betz, 1998; Levi et al., 1998). Later it was hypothesized that strychnine triggers the disappearance of GlyR from synapses (Rasmussen et al., 2002). In confirmation and addition to this view, our data for the first time functionally demonstrate that retrograde GFP–gephyrin transport and/or gephyrin–GlyR cotransport is directly sensitive to GlyR blockade. Moreover, consistent with our dual-channel time-lapse experiments, they provide another functional connection of GlyR and gephyrin cotransport in neurons.

Other transport complexes consist of neurotransmitter receptors and postsynaptic scaffold components (Kneussel, 2005). For instance, mLin2/CASK and GRIP1 comigrate in a kinesin-dependent manner with *N*-methyl-D-asparate (NMDA) or AMPA receptors, respectively (Setou et al., 2000, 2002). Hence, there has been an interest in the question of which motor system would drive a gephyrin–GlyR complex within neurons. Although a yeast two-hybrid screen identified the motor components Dlc-1 and -2 as gephyrin-binding partners (Fuhrmann et al., 2002), until now it was not clear whether these interactions point to actin- or microtubule-based transport reactions because DLCs

are components of both myosin and dynein complexes (King et al., 1996; Naisbitt et al., 2000). Applying both immunoprecipitation from intracellular fractions and immunocytochemistry, we demonstrate that both intracellular gephyrin and GlyR bind and colocalize with either DICs or DHCs, which are exclusive components of the dynein motor complex. Dynein motors are known to transport a large variety of cargo molecules in neurons and other cell types (Karki and Holzbaur, 1999; Harrison and King, 2000; Dujardin and Vallee, 2002); therefore, it is consistent that only a small proportion of dynein puncta colocalize with gephyrin at a given time. Remarkably, colocalized puncta were mainly found at nonsynaptic sites, a finding that suggests dynein motor complexes do not directly reach the postsynaptic specialization. This result resembles observations made for NMDA receptor synaptic delivery (Guillaud et al., 2003). A motor-cargo complex consisting of the microtubule-dependent kinesin KIF17 and the synaptic NMDA receptor subunit protein NR2B also colocalizes close to, but not at synaptic sites. Whether or not microtubule-based motors generally reach the postsynaptic site is currently unclear. However, actin filament–based motor systems, known to mediate short-distance transport (Langford, 1995), might contribute to cargo recruitment at synapses (Naisbitt et al., 2000; Wu et al., 2002; Kneussel, 2005).

Functional evidence that gephyrin recruitment depends on active transport through the dynein motor complex was given in different independent assays. First, active transport was confirmed by the lack of particle diffusion at high image acquisition rates. Second, loss-of-function experiments using dynamitin blockade of dynein in both HEK293 cells and neurons confirmed the association of gephyrin and dynein. In addition, by expressing a fluorescently labeled peptide that harbored the DLC-binding site of gephyrin (mRFP–gephyrin 181–243), we could show that this polypeptide is, on its own, highly mobile in neurons, indicating that it is able to associate with a molecular motor. Because short-term overexpression of this binding site was able to compete with retrograde GFP–gephyrin or GFP–GlyRβ transport in time-lapse experiments, but not with anterograde-dependent transport of clusters to distal dendrites, our data strongly indicate that GlyR–gephyrin complexes are functionally recruited via dynein.

Notably, our time-lapse analysis revealed that gephyrin and GlyRs move not only retrogradely but also in anterograde directions over time. Thus, it will be a challenge to identify the anterograde transport system that is required for gephyrin and/or GlyR recruitment toward the synapse. A GlyR–gephyrin–dynein triple transport complex is likely to contribute to the regulation of synaptic receptor number and the regulation of gephyrin scaffold, which in turn provides the platform for trapping of diffusing plasma membrane receptors. In this respect it is also important to understand whether dynein-mediated retrograde recruitment of the complex mainly represents receptor recycling processes, degradation of receptors, or both. Based on our observations that depolarization and/or receptor blockade influences transport parameters of the gephyrin–GlyR complex, it appears that cross talk between neuronal activity mechanisms and the neuronal transport machinery might be an important platform for the modulation of synaptic strength at inhibitory synapses.

Materials and methods

Constructs

The GFP–gephyrin fusion construct has been previously described (Fuhrmann et al., 2002). To generate YFP–gephyrin, the vector pEYFP-C1 (BD Biosciences) was restricted with BglII and treated with Klenow polymerase (Roche) in the presence of deoxyribonucleotide triphosphates to generate the pEYFP-C2 vector. The gephyrin complementary DNA was subsequently subcloned into pEYFP-C2 as a HindIII–KpnI fragment. To generate mRFP–gephyrin, the mRFP1 coding sequence was subcloned as a NheI–SacI fragment into GFP–gephyrin, thereby replacing GFP by mRFP1. To generate GFP–gephyrin 2–188, a PCR product encoding amino acids 2–188 of gephyrin was cloned as a HindIII–SalI fragment into pEGFP-C1 (BD Biosciences). For the generation of GFP–GlyRβ, a BglII restriction site was introduced after the signal peptide of a GlyRβ construct in pRK5. The GFP coding sequence was introduced as a BglII–BglII PCR product into this locus. Furthermore, the GlyRβ 3′-UTR was introduced into the PstI site of pRK5. To generate mRFP–gephyrin 181–243, a PCR product encoding mRFP1 was cloned as a NheI–SacI fragment into GFP–gephyrin 181–243 (Fuhrmann et al., 2002), thereby replacing GFP by mRFP1. GFP–dynamitin and Dynamitin–myc were obtained from R. Vallee, Columbia University, New York, NY. GFP–Shank 1 obtained from C. Sala, University of Milan, Milan, Italy. mRFP1 was obtained from R.Y. Tsien, University of California, San Diego, La Jolla, CA.

Antibodies

The following antibodies were used for immunoprecipitation and Western blotting: mouse anti-gephyrin (1:1,000; Synaptic Systems GmbH), mouse anti-gephyrin (1:250; BD Biosciences), rabbit anti-gephyrin (1:4,000; Alexis), mouse anti-GlyR, clone mAb4a (1:250; Synaptic Systems GmbH), rabbit anti-GlyR (1:100; Sigma-Aldrich), mouse anti-dynein intermediate chain (1:1,000; CHEMICON International, Inc.), mouse anti-dynein intermediate chain (1:1000; Sigma-Aldrich), and mouse anti-GluR2 (1:1,000; CHEMICON International, Inc.). The following antibodies were used for immunofluorescence: mouse anti-gephyrin (1:100; Synaptic Systems GmbH), rabbit anti-gephyrin (1:100; Qbiogene), mouse anti-GlyR, clone mAb4a (1:100; Synaptic Systems GmbH), goat anti-DHC, clone S-19 (1:100; Santa Cruz Biotechnology, Inc.), mouse anti-dynein intermediate chain (1:100; CHEMICON International, Inc.), rabbit anti-VIAAT (1:200; obtained from B. Gasnier, Centre National de la Recherche Scientifique, Paris, France; Dumoulin et al., 1999), mouse anti–α-tubulin (1:1,000; Sigma-Aldrich), mouse anti–γ-tubulin (1:100; Sigma-Aldrich), mouse anti-myc (1:100; Sigma-Aldrich), rabbit anti-myc (1:100; Sigma-Aldrich), mouse anti–synaptic vesicle (SV2; 1:100; Developmental Studies Hybridoma Bank), rabbit anti-synaptophysin (1:100; DakoCytomation), goat anti-synaptophysin (1:100; Santa Cruz Biotechnology, Inc.), and mouse anti-GM130 (1:100; Sigma-Aldrich). The following secondary antibodies were used: CY3-, CY2-, or CY5-conjugated donkey anti–goat, anti–mouse, or anti–rabbit (all 1:500; Dianova).

Sucrose gradient centrifugation

Brains of five postnatal day (P) 10 juvenile rats were homogenized in buffered sucrose solution containing 320 mM sucrose, 2 mM DTT, 1 mM EDTA, 1 mM EGTA, and 4 mM Hepes-KOH, pH 7.4, supplemented with proteinase inhibitor cocktail (Roche), 2 mM ATP, and 5 mM $MgCl_2$. The homogenate was centrifuged at 1000 *g* for 10 min (P1) and the resulting postnuclear supernatant further clarified at 10,000 *g* for 10 min (P2). Supernatant from this medium speed centrifugation was processed by another 160,000 *g* centrifugation step to collect small membrane organelles (P3). The pellet was resuspended in 1.5 ml of 2 M sucrose solution and subjected to a linear 0.3–2 M sucrose-density gradient centrifugation. The gradient was centrifuged at 160,000 *g* in a rotor (model SW49Ti; Beckman Coulter) for 12 h at 4°C. Fractions of ~750 μl were collected from the top of the gradient using a defractionator (Labconco). 20 μl of each fraction was used for SDS-PAGE and Western blotting.

Coimmunoprecipitation

Rat brains of five P10 animals were dissected in ice-cold PBS and homogenized in IM-Ac buffer, containing 20 mM Hepes, 100 mM KCl, 5 mM EGTA, and 5 mM $MgCl_2$, pH 7.2. The buffer was supplemented with proteinase inhibitor cocktail (Roche), 5 mM DTT, and 2 mM MgATP. The homogenate was clarified by centrifugation at 1000 *g* for 10 min and the postnuclear supernatant was used for the following steps. First, the supernatant was centrifuged at 10,000 *g* for 10 min to pellet large membrane

organelles (P2). The remaining supernatant was then centrifuged at 100,000 *g* to collect small membrane organelles (P3). Finally, remaining organelles and large protein complexes were pelleted at 400,000 *g* for 60 min (P4). After diaminopimelate cross-linking of antibodies to magnetic beads (Invitrogen), antigen from P3 or P4 fractions was immobilized, followed by extensive washing steps with either IM-Ac buffer or IM-Ac buffer containing 0.5% Triton X-100. Bound proteins were eluted by boiling in SDS-containing sample buffer and examined by Western blotting.

Cell culture, transfection, and microinjection

Primary cultures of hippocampal neurons were prepared from mice or rats at P0 and P1, as previously described (Fuhrmann et al., 2002; Neuhoff et al., 2005). Cells cultured between 4 and 12 d in vitro were used for transfection with either 4 μg Lipofectamine 2000 (Invitrogen) in serum-free medium or by a calcium phosphate coprecipitation protocol (Fuhrmann et al., 2002). For KCl experiments, hippocampal neurons were incubated in neurobasal/B27 medium containing 10 mM KCl for 1–3 min before fluorescent imaging. For FM-dye labeling of active synapses, cells were exposed to 15 μM FM4-64 for 1 min in 31.5 mM NaCl, 90 mM KCl, 5 mM Hepes, 1 mM $MgCl_2$, 2 mM $CaCl_2$, 30 mM glucose, and 50 μM DL-AP5. Imaging was performed in neurobasal/B27 medium containing 50 μM DL-AP5 and 10 μM of 6-cyano-7-nitroquinoxaline-2,3-dione. For GlyR or $GABA_AR$ blockade, neurons (12 d in vitro) expressing GFP–gephyrin were analyzed by time-lapse imaging in 10 mM Hepes and 10 mM KCl containing either 500 nM strychnine or 10 μM bicuculline. Drugs were added immediately before imaging. HEK293 cells were cultured on glass coverslips. For heterologous expression, cells were microinjected. Plasmids were purified using a complementary DNA purification kit (QIAGEN). Cells were kept in 10 mM of prewarmed Hepes buffer, pH 7.4, during the procedure. 30 ng/μl concentrations of DNA were microinjected into nuclei (Pepperkok et al., 1988) using a Transjector 5246 coupled with an Injectman system (both Eppendorf AG) at 70–100 hPa for 0.1–0.3 s. Visual control was obtained by the use of an inverted microscope equipped with a 63× long distance phase-contrast objective (Axiovert 35 and LD Plan Neofluar, respectively; Carl Zeiss MicroImaging, Inc.). For depolymerization of microtubules, the neurobasal/B27 medium of cultured hippocampal neurons was removed 3 h after transfection and stored separately. Cells were then incubated in fresh medium containing 10 μM nocodazole (Sigma-Aldrich) for 15 min, washed with PBS/10 mM glucose, and stored in the original neurobasal/B27 medium. After 24 h at 37°C/5% CO_2, cells were fixed and processed for immunocytochemistry.

Imaging and data analysis

Fluorescence imaging was performed with an inverted laser scanning confocal microscope (model TCS-SP2; Leica) using a 63× objective. For simultaneous multichannel fluorescence, images were taken in a sequential channel recording mode. Images from time-lapse experiments were taken with a TCS-SP2 microscope or an inverted fluorescent microscope (Axiovert 200M; Carl Zeiss MicroImaging, Inc.) combined with a charge-coupled device camera (SPOT RT-SE; Sony). Images were taken at various intervals ranging from every 30 to every 60 s. Cells at the microscope stage were temperature controlled (37°C) and either CO_2 controlled or kept in Hepes-buffered medium. For analysis of time-lapse data, dendrite length, size of puncta, and intensity histograms, Power Scan software TCS-NT (Leica), the analySIS software package 2.5 (Soft Imaging System GmbH), and the MetaVue 6.2r6 software (Universal Imaging Corp.) were used. Puncta were quantified using Scion Image 1.63 software (National Institutes of Health). The statistical significance of experiments was assessed with the *t* test.

Online supplemental material

Fig. S1 represents control figures for Figs. 4–6. Fig. S2 shows the effect of dynamitin on YFP–gephyrin localization in HEK293 cells. Fig. S3 is a control figure for Figs. 7 and 8. Fig. S4 shows that depolymerization of microtubules prevents the dominant-negative–induced loss of gephyrin clusters in neurons. Fig. S5 shows that mRFP–gephyrin 181–243 interferes with GFP–GlyRβ retrograde transport in neuronal dendrites. Video 1 shows the recruitment of GFP–gephyrin as shown in Fig. 2. Video 2 shows the recruitment of GFP–gephyrin toward and/or from FM4-64–positive presynaptic terminal boutons, as shown in Fig. 3. Video 3 shows the cotransport of GFP–GlyRβ and mRFP–gephyrin, as shown in Fig. 5 A. Online supplemental material is available at http://www.jcb.org/cgi/content/full/jcb.200506066/DC1.

We thank R. Vallee and B. Sodeik for the GFP–dynamitin and dynamitin–myc constructs and C. Sala and H.J. Kreienkamp for the GFP–Shank1 construct. We further thank B. Gasnier for kindly providing the VIAAT-specific antibody, R.Y. Tsien for the mRFP1 vector, and S. Plant for excellent technical assistance.

This work was supported by the University of Hamburg and grants KN-556/1-1, KN-556/1-2, and SFB444/B7 from the Deutsche Forschungsgemeinschaft to M. Kneussel.

Submitted: 16 June 2005
Accepted: 27 December 2005

References

Ackermann, M., and A. Matus. 2003. Activity-induced targeting of profilin and stabilization of dendritic spine morphology. *Nat. Neurosci.* 6:1194–1200.

Ahmad, F.J., C.J. Echeverri, R.B. Vallee, and P.W. Baas. 1998. Cytoplasmic dynein and dynactin are required for the transport of microtubules into the axon. *J. Cell Biol.* 140:391–401.

Burkhardt, J.K., C.J. Echeverri, T. Nilsson, and R.B. Vallee. 1997. Overexpression of the dynamitin (p50) subunit of the dynactin complex disrupts dynein-dependent maintenance of membrane organelle distribution. *J. Cell Biol.* 139:469–484.

Choquet, D., and A. Triller. 2003. The role of receptor diffusion in the organization of the postsynaptic membrane. *Nat. Rev. Neurosci.* 4:251–265.

Danglot, L., P. Rostaing, A. Triller, and A. Bessis. 2004. Morphologically identified glycinergic synapses in the hippocampus. *Mol. Cell. Neurosci.* 27:394–403.

Dong, H., R.J. O'Brien, E.T. Fung, A.A. Lanahan, P.F. Worley, and R.L. Huganir. 1997. GRIP: a synaptic PDZ domain-containing protein that interacts with AMPA receptors. *Nature*. 386:279–284.

Dujardin, D.L., and R.B. Vallee. 2002. Dynein at the cortex. *Curr. Opin. Cell Biol.* 14:44–49.

Dumoulin, A., P. Rostaing, C. Bedet, S. Levi, M.F. Isambert, J.P. Henry, A. Triller, and B. Gasnier. 1999. Presence of the vesicular inhibitory amino acid transporter in GABAergic and glycinergic synaptic terminal boutons. *J. Cell Sci.* 112:811–823.

Essrich, C., M. Lorez, J.A. Benson, J.M. Fritschy, and B. Luscher. 1998. Postsynaptic clustering of major GABAA receptor subtypes requires the gamma 2 subunit and gephyrin. *Nat. Neurosci.* 1:563–571.

Feany, M.B., S. Lee, R.H. Edwards, and K.M. Buckley. 1992. The synaptic vesicle protein SV2 is a novel type of transmembrane transporter. *Cell*. 70:861–867.

Fischer, M., S. Kaech, U. Wagner, H. Brinkhaus, and A. Matus. 2000. Glutamate receptors regulate actin-based plasticity in dendritic spines. *Nat. Neurosci.* 3:887–894.

Fuhrmann, J.C., S. Kins, P. Rostaing, O. El Far, J. Kirsch, M. Sheng, A. Triller, H. Betz, and M. Kneussel. 2002. Gephyrin interacts with Dynein light chains 1 and 2, components of motor protein complexes. *J. Neurosci.* 22:5393–5402.

Giesemann, T., G. Schwarz, R. Nawrotzki, K. Berhorster, M. Rothkegel, K. Schluter, N. Schrader, H. Schindelin, R.R. Mendel, J. Kirsch, and B.M. Jockusch. 2003. Complex formation between the postsynaptic scaffolding protein gephyrin, profilin, and Mena: a possible link to the microfilament system. *J. Neurosci.* 23:8330–8339.

Guillaud, L., M. Setou, and N. Hirokawa. 2003. KIF17 dynamics and regulation of NR2B trafficking in hippocampal neurons. *J. Neurosci.* 23:131–140.

Guzik, B.W., and L.S. Goldstein. 2004. Microtubule-dependent transport in neurons: steps towards an understanding of regulation, function and dysfunction. *Curr. Opin. Cell Biol.* 16:443–450.

Harrison, A., and S.M. King. 2000. The molecular anatomy of dynein. *Essays Biochem.* 35:75–87.

Hirokawa, N., and R. Takemura. 2005. Molecular motors and mechanisms of directional transport in neurons. *Nat. Rev. Neurosci.* 6:201–214.

Holzbaur, E.L. 2004. Motor neurons rely on motor proteins. *Trends Cell Biol.* 14:233–240.

Karki, S., and E.L. Holzbaur. 1999. Cytoplasmic dynein and dynactin in cell division and intracellular transport. *Curr. Opin. Cell Biol.* 11:45–53.

Kennedy, M.B. 2000. Signal-processing machines at the postsynaptic density. *Science*. 290:750–754.

King, S.J., and T.A. Schroer. 2000. Dynactin increases the processivity of the cytoplasmic dynein motor. *Nat. Cell Biol.* 2:20–24.

King, S.M., E. Barbarese, J.F. Dillman III, R.S. Patel-King, J.H. Carson, and K.K. Pfister. 1996. Brain cytoplasmic and flagellar outer arm dyneins share a highly conserved Mr 8,000 light chain. *J. Biol. Chem.* 271:19358–19366.

Kirsch, J., and H. Betz. 1995. The postsynaptic localization of the glycine receptor-associated protein gephyrin is regulated by the cytoskeleton. *J. Neurosci.* 15:4148–4156.

Kirsch, J., and H. Betz. 1998. Glycine-receptor activation is required for receptor clustering in spinal neurons. *Nature*. 392:717–720.

Kneussel, M. 2005. Postsynaptic scaffold proteins at non-synaptic sites. *EMBO Rep.* 6:22–27.

Kneussel, M., and H. Betz. 2000. Clustering of inhibitory neurotransmitter receptors at developing postsynaptic sites: the membrane activation model. *Trends Neurosci.* 23:429–435.

Kneussel, M., J.H. Brandstatter, B. Laube, S. Stahl, U. Muller, and H. Betz. 1999. Loss of postsynaptic GABA(A) receptor clustering in gephyrin-deficient mice. *J. Neurosci.* 19:9289–9297.

Langford, G.M. 1995. Actin- and microtubule-dependent organelle motors: interrelationships between the two motility systems. *Curr. Opin. Cell Biol.* 7:82–88.

Levi, S., C. Vannier, and A. Triller. 1998. Strychnine-sensitive stabilization of postsynaptic glycine receptor clusters. *J. Cell Sci.* 111:335–345.

Li, Z., and M. Sheng. 2003. Some assembly required: the development of neuronal synapses. *Nat. Rev. Mol. Cell Biol.* 4:833–841.

Lorenzo, L.E., A. Barbe, and H. Bras. 2004. Mapping and quantitative analysis of gephyrin cytoplasmic trafficking pathways in motoneurons, using an optimized transmission electron microscopy color imaging (TEMCI) procedure. *J. Neurocytol.* 33:241–249.

Marrs, G.S., S.H. Green, and M.E. Dailey. 2001. Rapid formation and remodeling of postsynaptic densities in developing dendrites. *Nat. Neurosci.* 4:1006–1013.

Moss, S.J., and T.G. Smart. 2001. Constructing inhibitory synapses. *Nat. Rev. Neurosci.* 2:240–250.

Naisbitt, S., J. Valtschanoff, D.W. Allison, C. Sala, E. Kim, A.M. Craig, R.J. Weinberg, and M. Sheng. 2000. Interaction of the postsynaptic density-95/guanylate kinase domain-associated protein complex with a light chain of myosin-V and dynein. *J. Neurosci.* 20:4524–4534.

Neuhoff, H., M. Sassoe-Pognetto, P. Panzanelli, C. Maas, W. Witke, and M. Kneussel. 2005. The actin-binding protein profilin I is localized at synaptic sites in an activity-regulated manner. *Eur. J. Neurosci.* 21:15–25.

Oakley, B.R., and Y.N. Akkari. 1999. Gamma-tubulin at ten: progress and prospects. *Cell Struct. Funct.* 24:365–372.

Passafaro, M., C. Sala, M. Niethammer, and M. Sheng. 1999. Microtubule binding by CRIPT and its potential role in the synaptic clustering of PSD-95. *Nat. Neurosci.* 2:1063–1069.

Pepperkok, R., C. Schneider, L. Philipson, and W. Ansorge. 1988. Single cell assay with an automated capillary microinjection system. *Exp. Cell Res.* 178:369–376.

Quinlan, E.M., and S. Halpain. 1996. Emergence of activity-dependent, bidirectional control of microtubule-associated protein MAP2 phosphorylation during postnatal development. *J. Neurosci.* 16:7627–7637.

Rasmussen, H., T. Rasmussen, A. Triller, and C. Vannier. 2002. Strychnine-blocked glycine receptor is removed from synapses by a shift in insertion/degradation equilibrium. *Mol. Cell. Neurosci.* 19:201–215.

Saito, N., Y. Okada, Y. Noda, Y. Kinoshita, S. Kondo, and N. Hirokawa. 1997. KIFC2 is a novel neuron-specific C-terminal type kinesin superfamily motor for dendritic transport of multivesicular body-like organelles. *Neuron*. 18:425–438.

Samson, F., J.A. Donoso, I. Heller-Bettinger, D. Watson, and R.H. Himes. 1979. Nocodazole action on tubulin assembly, axonal ultrastructure and fast axoplasmic transport. *J. Pharmacol. Exp. Ther.* 208:411–417.

Sanes, J.R., and J.W. Lichtman. 2001. Induction, assembly, maturation and maintenance of a postsynaptic apparatus. *Nat. Rev. Neurosci.* 2:791–805.

Schmitt, B., P. Knaus, C.M. Becker, and H. Betz. 1987. The Mr 93,000 polypeptide of the postsynaptic glycine receptor complex is a peripheral membrane protein. *Biochemistry*. 26:805–811.

Setou, M., T. Nakagawa, D.H. Seog, and N. Hirokawa. 2000. Kinesin superfamily motor protein KIF17 and mLin-10 in NMDA receptor-containing vesicle transport. *Science*. 288:1796–1802.

Setou, M., D.H. Seog, Y. Tanaka, Y. Kanai, Y. Takei, M. Kawagishi, and N. Hirokawa. 2002. Glutamate-receptor-interacting protein GRIP1 directly steers kinesin to dendrites. *Nature*. 417:83–87.

Sola, M., M. Kneussel, I.S. Heck, H. Betz, and W. Weissenhorn. 2001. X-ray crystal structure of the trimeric N-terminal domain of gephyrin. *J. Biol. Chem.* 276:25294–25301.

Sola, M., V.N. Bavro, J. Timmins, T. Franz, S. Ricard-Blum, G. Schoehn, R.W. Ruigrok, I. Paarmann, T. Saiyed, G.A. O'Sullivan, et al. 2004. Structural basis of dynamic glycine receptor clustering by gephyrin. *EMBO J.* 23:2510–2519.

Star, E.N., D.J. Kwiatkowski, and V.N. Murthy. 2002. Rapid turnover of actin in dendritic spines and its regulation by activity. *Nat. Neurosci.* 5:239–246.

Washbourne, P., J.E. Bennett, and A.K. McAllister. 2002. Rapid recruitment of NMDA receptor transport packets to nascent synapses. *Nat. Neurosci.* 5:751–759.

Wu, H., J.E. Nash, P. Zamorano, and C.C. Garner. 2002. Interaction of SAP97 with minus-end-directed actin motor myosin VI. Implications for AMPA receptor trafficking. *J. Biol. Chem.* 277:30928–30934.

Wyszynski, M., E. Kim, F.C. Yang, and M. Sheng. 1998. Biochemical and immunocytochemical characterization of GRIP, a putative AMPA receptor anchoring protein, in rat brain. *Neuropharmacology*. 37:1335–1344.